

ГОРНАЯ МЕХАНИКА. ГОРНЫЕ МАШИНЫ И ТРАНСПОРТ

DOI: 10.21440/0536-1028-2021-5-87-98

Theoretical justification of the roller press force parameters

Oleg A. Dorofeev¹, Evgenii A. Shishkin^{1*}, Anatolii A. Serebrennikov²,
Dmitrii E. Abramenzov³

¹ Pacific National University, Khabarovsk, Russia

² Tyumen Industrial University, Tyumen, Russia

³ Novosibirsk State University of Architecture and Civil Engineering, Novosibirsk, Russia

*e-mail: 004655@pnu.edu.ru

Abstract

Introduction. Despite being underused due to its low heat transfer, silt coal is an attractive thermal energy source. Silt coal is molded into briquettes by press machines, mostly roller presses marked by high reliability and relatively simple design, to increase heat transfer. The quality of the resulting briquette depends on the pressing force of the working elements.

Research objective is to determine the relationship between the force parameters of the press and the physical and mechanical properties of the pressed material.

Methods of research. The interaction between the rollers and the pressed material is analyzed in the deformation zone pressing area. A plane problem is solved considering the uniform distribution of material pressure across the roller generatrices. An elastic-visco-plastic rheological model is used to describe the stress-strain state of the pressed material. The model best reflects the behavior of an actual physical medium.

Results. For the adopted rheological model, analytical dependencies between the pressure put on the pressed material and the press angle have been obtained for various stages of material deformation. An analytical relation between the pressing force, the moment of resistance to roller rotation, press design parameters, and the physical and mechanical properties of the pressed material has been determined.

Conclusions. The obtained dependencies will contribute to a more conscious choice of the press power equipment that ensures roller compression and the drive of the required power to produce high-quality briquettes.

Keywords: roller press; design parameters; briquette; pressing force; moment of resistance to rotation; elastic-visco-plastic model; press angle.

Introduction. Concentrate and waste are the products of rock beneficiation in opencast coal mines. Silt coal is usually stored in tailings storage facilities [1]. Recently, there has been a growing tendency to process coal-bearing waste [2, 3]. Silt coal is molded into briquettes to increase heat transfer [4, 5]. The process is mostly performed by roller presses marked by high reliability and relatively simple design [6, 7]. The press force parameters must ensure the production of the required quality [8, 9]. This research aims to determine the relationship between the force parameters of the press and the physical and mechanical properties of the pressed material.

Methods of research. The following assumptions were made while studying the process of silt coal interaction with the rollers of the press:

1. The force acting in feed and motion zones consists mainly of silt coal friction (sliding friction) against the roller surface and pressure caused by the gravity of silt coal with the bulk density and located above the pressing area [10]. These forces are tiny and incomparable with the forces acting in the pressing area, and therefore can be neglected. So, in the deformation zone pressing area, the rollers are exposed to the main force action from the silt coal.

2. Roller surface pressure along any generatrix is evenly distributed [11], which means that a plane problem is solved.

3. In the pressing area, the layers of the material stop sliding against each other and against the surface of the rollers [12] due to a significant increase in the material-rollers friction. As a result, the elementary horizontal layer of the material in the pressing area does not change its orientation and shifts down vertically. Material is therefore deformed under the conditions of horizontal uniaxial compression in the pressing area.

4. The material in the pressing area is displayed as a rheological model. Its parameters are defined by experiment according to the existing methods [13]. Press angle α_{press} is also regarded as known from the uniaxial compression tests.

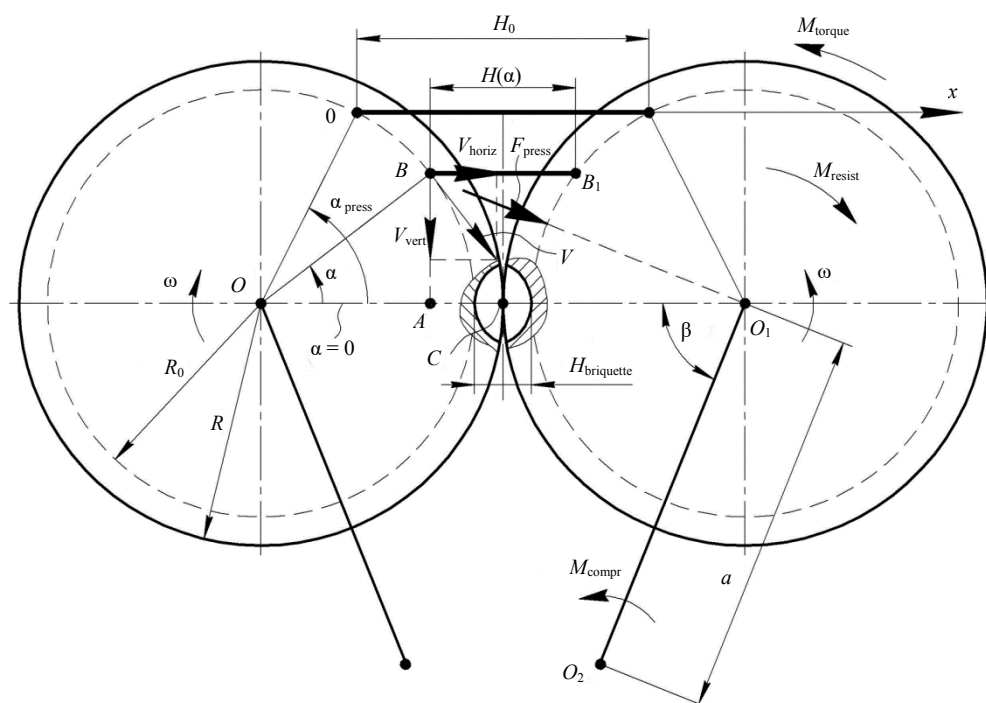


Fig. 1. Scheme of interaction of press rollers with compacted waste
Рис. 1. Схема взаимодействия валков пресса с уплотняемыми отходами

Considering the accepted assumptions, the scheme of roller-pressed material interaction may be represented as shown in Figure 1.

Force F_{press} from the deformed material, which creates the roller compression inhibiting moment of thrust about the O_2 axis, meets the optimal force of pressing for the particular material, as far as the briquette quality is concerned [14]:

$$F_{\text{press}} a = M_{\text{compr}},$$

where M_{compr} is the moment of compression created by the power equipment of the press about the O_2 axis, $\text{N} \cdot \text{m}$; a is the distance between the bearing axis O_2 and the roller axis of rotation O_1 , m.

Under $F_{\text{press}} a > M_{\text{compr}}$ the required quality of briquettes will not be achieved. Under $F_{\text{press}} a < M_{\text{compr}}$, the required quality of briquettes will be achieved, but the capacity of the power equipment will not be used effectively.

So, by the pressing force, we shall mean force F_{press} directed along the roller radius. On arm a , F_{press} creates the moment of thrust about the O_2 axis that is as big as all the radial forces exerted on the surface of the roller in the pressing area.

The modified roller radius, m , is determined by the formula [15]:

$$R_0 = R - \frac{H_{\text{briquette}}}{2},$$

where R is the roller radius, m ; $H_{\text{briquette}}$ is the average thickness of the finished briquette, m .

The briquette compaction ratio is determined by the formula:

$$K_{\text{comp}} = \frac{\rho_{\text{briquette}}}{\rho_{\text{bulk}}} = \frac{H_0}{H_{\text{briquette}}}, \quad (1)$$

where $\rho_{\text{briquette}}$ is the density of the finished briquette, kg/m^3 ; ρ_{bulk} is the bulk density, kg/m^3 ; H_0 is the distance between the generatrices of rollers along the upper boundary of the pressing area, m .

It follows from the right triangle AOB (Figure 1) that:

$$\cos \alpha_{\text{press}} = \frac{AO}{BO} = \left(R_0 - \frac{H_0 - H_{\text{briquette}}}{2} \right) R_0^{-1}. \quad (2)$$

Considering equations (1) and (2), we obtain the press angle formula:

$$\alpha_{\text{press}} = \arccos \left[1 - \frac{(K_{\text{comp}} - 1)H_{\text{briquette}}}{2R_0} \right].$$

Let us consider the deformation of the elementary rod BB_1 (Figure 1). Angle α is read from the line which connects the roller oscillation axes. Axis Ox is directed alongside the deformed element with a reference rigidly bound to the left edge of the element (moving frame). The deformation begins to be counted when the length of the deformed element is H_0 , which agrees with the angle $\alpha = \alpha_{\text{press}}$. So, the initial conditions will be as follows: at $x = 0$: pressure on the element $p = 0$, element length $H = H_0$, angle $\alpha = \alpha_{\text{press}}$.

The linear speed of any point on the roller surface is

$$V = \omega R_0 = \text{const},$$

where ω is the rotational angular velocity of the roller, s^{-1} .

Let us break the linear velocity down into two components: the horizontal V_{horiz} and vertical V_{vert} (Figure 1). Then the approach velocity of the two points B and B_1 (lines BB_1 and OO_1 are parallel) is:

$$V(\alpha) = 2V_{\text{horiz}} = 2\omega R_0 \sin \alpha. \quad (3)$$

Velocity $V(\alpha)$ agrees with the speed of material deformation in the pressing area:

$$V(\alpha) = x'(\alpha).$$

Following Figure 1, the length of the deformed element at an arbitrary moment is

$$H(\alpha) = 2AC = 2\left(R_0 - AO + \frac{H_{\text{briquette}}}{2}\right).$$

After the right triangle AOB has been considered, let us rearrange the equation into the following form:

$$H(\alpha) = 2R_0(1 - \cos \alpha) + H_{\text{briquette}}. \quad (4)$$

BB_1 deformation at an arbitrary moment is

$$x(\alpha) = H(\alpha_{\text{press}}) - H(\alpha).$$

Considering (4) we get

$$x(\alpha) = 2R_0(\cos \alpha - \cos \alpha_{\text{press}}). \quad (5)$$

The Bingham body (Figure 2) best reflects the behavior of the actual physical medium, so it is used in a rheological model.

Ideal elastic and elastoplastic are the two stages of material deformation.

Elastic limit deformation x_1 corresponds to the moment when the pressure becomes equal to the yield stress $p = \sigma_{\text{yield}}$ (the moment of the Saint-Venant's body action), while x_{final} is the final deformation (Figure 2).

At the ideal elastic stage of material deformation, the pressure is lower than the yield stress: $p < \sigma_{\text{yield}}$.

Elastic deformations $x = x_y$ are typical for this stage, and only Hooke's body resists deformation p_b , which is equal to pressure p .

Pressure

$$p(\alpha) = bx(\alpha),$$

where b is the material's modulus of rigidity, N/m^3 .

Considering equation (5) we obtain

$$p(\alpha) = 2R_0b(\cos \alpha - \cos \alpha_{\text{press}}). \quad (6)$$

When the pressure p reaches the value of the yield stress σ_{yield} , equation (6) will become:

$$p(\alpha_1) = \sigma_T = 2R_0b(\cos \alpha_1 - \cos \alpha_{\text{press}}). \quad (7)$$

Let us derive angle α_1 from equation (7):

$$\alpha_1 = \arccos\left(\frac{\sigma_T}{2R_0b} + \cos \alpha_{\text{press}}\right).$$

Let us refer to angle α_1 corresponding to deformation x_1 as the angle of the elastic limit deformation.

At the elastoplastic stage of material deformation, pressure does not exceed the yield stress $p \geq \sigma_{\text{yield}}$.

The following dependencies are typical for this stage:

$$\begin{cases} p = p_b = \sigma_{\text{yield}} + p_{\mu}; \\ p_{\mu} = \mu x'_{\text{plastic}}; \\ p_b = bx_y; \\ x = x_y + x_{\text{plastic}}, \end{cases}$$

where x_{plastic} is the plastic strain, m; p_{μ} is the resistance to deformation, N/m², by the Newton's body; μ is the coefficient of dynamic viscosity of the material, N · c/m³.

Considering

$$x'_{\text{plastic}} = x' - \frac{p'}{b},$$

the differential equation of the behavior of the model under $p \geq \sigma_{\text{yield}}$ will become

$$p'(\alpha) + \frac{b}{\mu} p(\alpha) = bx'(\alpha) + \frac{b}{\mu} \sigma_{\text{yield}}.$$

Since $x'(\alpha) = V(\alpha)$, then considering equation (3) and having denoted $b/\mu = \tau$, we get:

$$p'(\alpha) + \tau p(\alpha) = 2b\omega R_0 \sin \alpha + \tau \sigma_{\text{yield}}. \quad (8)$$

Equation (8) is the first-order linear differential equation, the general solution to which is as follows:

$$p(\alpha) = \frac{2bR_0\omega}{1 + \tau^2} (\tau \sin \alpha - \cos \alpha) + \sigma_{\text{yield}} + C \exp(-\tau\alpha).$$

Having denoted

$$K = \frac{2bR_0\omega}{1 + \tau^2},$$

we get

$$p(\alpha) = K(\tau \sin \alpha - \cos \alpha) + \sigma_{\text{yield}} + C \exp(-\tau\alpha).$$

The integration constant C is derived from the condition $p(\alpha_1) = \sigma_{\text{yield}}$:

$$C = K(\cos \alpha_1 - \tau \sin \alpha_1) \exp(\tau\alpha_1).$$

Having denoted

$$A = (\cos \alpha_1 - \tau \sin \alpha_1) \exp(\tau\alpha_1),$$

we get

$$C = KA.$$

Then the partial solution of the differential equation (8) becomes:

$$p(\alpha) = K(\tau \sin \alpha - \cos \alpha) + \sigma_T + KA \exp(-\tau \alpha). \quad (9)$$

Let us break pressure $p(\alpha)$ acting on the roller surface in a point B_1 from the direction of the horizontally deformed element into two components: radial $p_r(\alpha)$ and circumferential $p_\tau(\alpha)$ (Figure 3).

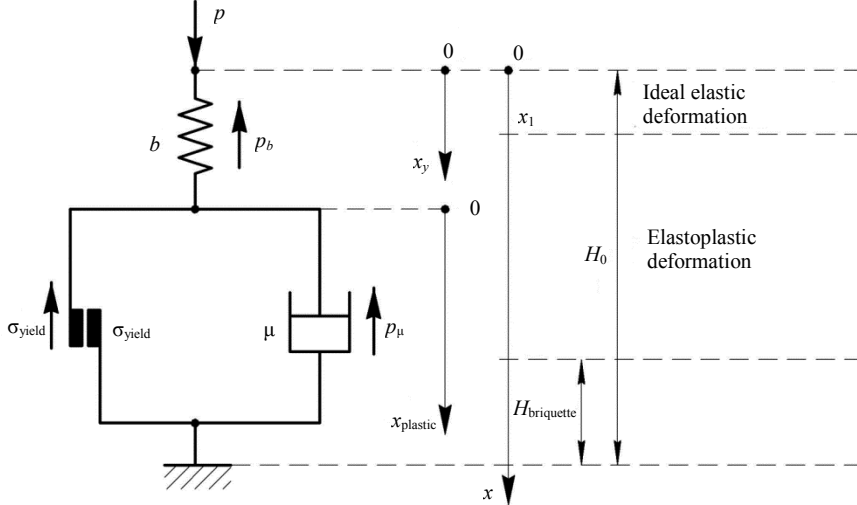


Fig. 2. Rheological model of the compacted material
Рис. 2. Реологическая модель уплотняемого материала

The radial component $p_r(\alpha)$ creates the thrust force aiming at pulling the rollers apart, while the circumferential component $p_\tau(\alpha)$ counteracts the roller drive torque:

$$p_r(\alpha) = p(\alpha) \cos \alpha; \quad p_\tau(\alpha) = p(\alpha) \sin \alpha. \quad (10)$$

Let us select an infinitesimal arc dl on the roller surface (Figure 3); along the arc, the force can be considered constant. Infinitesimal increment of the angle α equal to $d\alpha$ corresponds to the arc. The relation between the arc and the angle is expressed by the ratio:

$$dl = R_0 d\alpha. \quad (11)$$

Then the elementary radial force $P_r(\alpha)$ acting on the surface of the roller with dlB area, considering equations (10) and (11) is

$$P_r(\alpha) = p(\alpha) \cos \alpha BR_0 d\alpha, \quad (12)$$

where B is the width of the rolling face, m.

Force (12) creates the elementary moment of thrust $dm_{\text{thrust}}(\alpha)$ about axis O_2 equal to

$$dm_{\text{thrust}}(\alpha) = p(\alpha) \cos \alpha BR_0 L(\alpha) d\alpha, \quad (13)$$

where $L(\alpha)$ is the arm of the elementary radial force $P_r(\alpha)$, m.

It follows from the right triangle O_1O_2C (Figure 3) that:

$$L(\alpha) = a \sin(\alpha + \beta). \quad (14)$$

Considering expression (14), the equation of the elementary moment of thrust (13) becomes as follows:

$$dm_{\text{thrust}}(\alpha) = p(\alpha) \cos \alpha BR_0 a \sin(\alpha + \beta) d\alpha.$$

The value of the complete moment of thrust will be expressed by the following integral:

$$M_{\text{thrust}} = \int_{\alpha_{\text{press}}}^0 dm_{\text{thrust}}(\alpha) = aBR_0 \int_{\alpha_{\text{press}}}^0 p(\alpha) \cos \alpha \sin(\alpha + \beta) d\alpha.$$

Finally, the pressing force, according to the definition, will be

$$F_{\text{press}} = \frac{M_{\text{thrust}}}{a} = BR_0 \int_{\alpha_{\text{press}}}^0 p(\alpha) \cos \alpha \sin(\alpha + \beta) d\alpha. \quad (15)$$

Similarly, elementary circumferential force $P_{\tau}(\alpha)$ acting on the surface of the roller with the area dlB , considering (10) and (11), is

$$P_{\tau}(\alpha) = p(\alpha) \sin \alpha BR_0 d\alpha. \quad (16)$$

Elementary torque $dm_c(\alpha)$ from the action of force (16) about the axis O_1 is

$$dm_c(\alpha) = BR_0^2 p(\alpha) \sin \alpha d\alpha.$$

The complete moment of resistance counteracting the roller rotation about the axis O_1 (Figure 1) is found by summing all elementary moments in the pressing area:

$$M_{\text{resist}} = \int_{\alpha_{\text{press}}}^0 dm_c(\alpha) = BR_0^2 \int_{\alpha_{\text{press}}}^0 p(\alpha) \sin \alpha d\alpha. \quad (17)$$

For the press drive calculation, it should be taken into account that the moment of resistance M_{resist} counteracts the rotation of only one roller.

By substituting equations (6) and (9) into equation (15), we get:

$$F_{\text{press}} = BR_0 \left[\int_{\alpha_{\text{press}}}^{\alpha_1} 2R_0 b (\cos \alpha - \cos \alpha_{\text{press}}) \cos \alpha \sin(\alpha + \beta) d\alpha + \int_{\alpha_1}^0 (K \tau \sin \alpha - K \cos \alpha + \sigma_T + KA \exp(-\tau \alpha)) \cos \alpha \sin(\alpha + \beta) d\alpha \right].$$

After integration, we obtain the pressing force formula:

$$\begin{aligned}
 F_{\text{press}} = BR_0 \left\{ R_0 b \left[\frac{\cos(\alpha_1 - \beta) - \cos(\alpha_{\text{press}} - \beta)}{2} - \frac{\cos(3\alpha_1 + \beta) - \cos(3\alpha_{\text{press}} + \beta)}{6} - \right. \right. \\
 \left. \left. - \cos(\alpha_1 + \beta) + \cos(\alpha_{\text{press}} + \beta) + \right. \right. \\
 \left. \left. + \frac{\cos \alpha_{\text{press}} [\cos(2\alpha_1 + \beta) - \cos(2\alpha_{\text{press}} + \beta) - 2\sin\beta(\alpha_1 - \alpha_{\text{press}})]}{2} \right] + \right. \\
 \left. + \frac{K\tau}{12} [\sin(3\alpha_1 + \beta) - 3\sin(\alpha_1 - \beta) - 4\sin\beta] - \frac{K}{12} [\cos(3\alpha_1 + \beta) + 6\cos(\alpha_1 + \beta) - \right. \\
 \left. - 3\cos(\alpha_1 - \beta) - 4\cos\beta] + \frac{\sigma_{\text{yield}}}{4} [\cos(2\alpha_1 + \beta) - 2\alpha_1 \sin\beta - \cos\beta] + \right. \\
 \left. + \frac{KA}{2} \left[\exp(-\tau\alpha_1) \left(\frac{\tau \sin(2\alpha_1 + \beta) + 2\cos(2\alpha_1 + \beta)}{\tau^2 + 4} + \frac{\sin\beta}{\tau} \right) - \frac{\tau \sin\beta + 2\cos\beta}{\tau^2 + 4} - \frac{\sin\beta}{\tau} \right] \right\}. \quad (18)
 \end{aligned}$$

By substituting equations (6) and (9) into equation (17), we get:

$$\begin{aligned}
 M_{\text{resist}} = BR_0^2 \left[\int_{\alpha_{\text{press}}}^{\alpha_1} 2R_0 b (\cos \alpha - \cos \alpha_{\text{press}}) \sin \alpha d\alpha + \right. \\
 \left. + \int_{\alpha_1}^0 (K\tau \sin \alpha - K \cos \alpha + \sigma_T + KA \exp(-\tau\alpha)) \sin \alpha d\alpha \right].
 \end{aligned}$$

After integration, we obtain the formula for the moment of resistance to roller rotation:

$$\begin{aligned}
 M_{\text{resist}} = BR_0^2 \left\{ -R_0 b (\cos \alpha_{\text{press}} - \cos \alpha_1)^2 + \frac{K\tau}{4} (\sin 2\alpha_1 - 2\alpha_1) + \frac{K}{2} \sin^2 \alpha_1 + \right. \\
 \left. + \sigma_{\text{yield}} (\cos \alpha_1 - 1) + KA \frac{\exp(-\tau\alpha_1) (\tau \sin \alpha_1 - \cos \alpha_1) - 1}{\tau^2 + 1} \right\}. \quad (19)
 \end{aligned}$$

Results. The pressing force obtained from equation (18) makes it possible to determine the value of the moment of compression M_{compr} that balances torque F_{press} from the deformed material. It will help to select the size of the hydraulic cylinder to create the proper pressing force.

The moment of resistance M_{resist} found from (19) is equal to the required torque M_{torque} created by the press drive about the axis O1 (Figure 1), which helps to select the size of the drive.

Conclusions. The present paper introduces a condition for the proper quality of a briquette in terms of the pressing force value.

A relationship is determined between the press geometry and the deformed material.

The laws of material pressure change depending on its physical and mechanical characteristics for different stages of deformation have been obtained.

As a result, the dependencies between the pressing force, moment of resistance, the physical and mechanical characteristics of the material, and rollers geometry were found. By defining the pressing force value, it is possible to choose press power

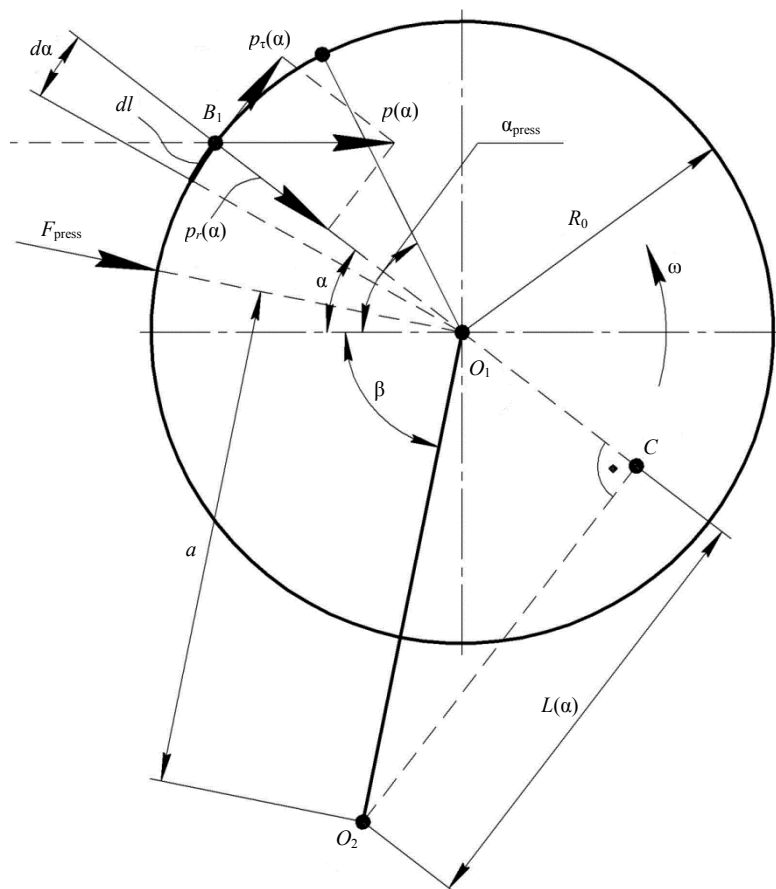


Fig. 3. Scheme of the effect of deformable material on the roller
Рис. 3. Схема воздействия деформируемого материала на валок

equipment aimed at ensuring the roller compression, on reasonable grounds. In turn, the value of the moment of resistance to roller rotation from the deformed material will make it possible to select a drive with the proper power to obtain briquettes of the proper quality, assessed by the compaction coefficient.

REFERENCES

1. Bazhin V. Iu., Kuskov V. B., Kuskova Ia. V. Problems of using unclaimed coal and other carbon-containing materials as energy briquettes. *Ugol = Coal*. 2019; 4(1117): 50–54. (In Russ.).
2. Kuskov V. B., Bazhin V. Iu. Use of various types of carbon-containing raw materials to produce thermal energy. *Zapiski Gornogo Instituta = Journal of Mining Institute*. 2016; 220: 582–586. (In Russ.).
3. Xu R., Dai B., Wang W., Schenk J., Xue Z. Effect of iron ore type on the thermal behaviour and kinetics of coal-iron ore briquettes during coking. *Fuel Processing Technology*. 2018; 173: 11–20. Available from: doi: 10.1016/j.fuproc.2018.01.006
4. Nikishanin M. S., Zagrutdinov R. Sh., Senachin P. K. Briquetting of local fuels and waste for energy supply systems in rural areas. *Polzunovskii vestnik = Polzunovsky Bulletin*. 2016; 1: 88–95. (In Russ.)

5. Manyuchi M., Mbohwa C., Muzenda E. Value addition of coal fines and sawdust to briquettes using molasses as a binder. *South African Journal of Chemical Engineering*. 2018; 26: 70–73. Available from: doi: 10.1016/j.sajce.2018.09.004
6. Efimov V. I., Nikulin I. B. Production of briquettes from coal sludge of concentration plants. *Gornyi informatsionno-analiticheskii bulletin (nauchno-tekhnicheskii zhurnal) = Mining Informational and Analytical Bulletin (scientific and technical journal)*. 2012; 4–10: 26–32. (In Russ.)
7. Fehse F., Rosin K., Hans-Werner S., Kim R., Spöttle M., Repke J.-U. Influence of briquetting and coking parameters on the lump coke production using non-caking coals. *Fuel*. 2017; 203: 915–923. Available from: doi: 10.1016/j.fuel.2017.05.002
8. Bolshakov V. I., Maimur B. N., Baiul K. V. Scientific foundations of technology and equipment for briquetting industrial waste. *Chernaia metallurgiya. Bulletin nauchno-tekhnicheskoi i ekonomicheskoi informatsii = Ferrous metallurgy. Bulletin of scientific, technical and economic information*. 2009; 8(1316): 54–59. (In Russ.)
9. Wilczyński D., Berdychowski M., Talaśka K., Wojtkowiak D. Experimental and numerical analysis of the effect of compaction conditions on briquette properties. *Fuel*. 2021; 288: 119613. Available from: doi: 10.1016/j.fuel.2020.119613
10. Noskov V. A., Maimur M. N., Petrenko V. I. Development of technology for the production of coke briquettes at JSC Balgeyoks. *Metallurgicheskaya i gornorudnaya promyshlennost = Metallurgical and mining industry*. 2005; 3: 108–111. (In Russ.)
11. Diakonov O. M. Force calculation of the process of briquetting powder, chip and other bulk materials. *Litie i metallurgiya = Foundry Production and Metallurgy*. 2019; 3: 118–125. (In Russ.)
12. Baiul K., Khudyakov A., Vashchenko S., Krot P., Solodka N. The experimental study of compaction parameters and elastic after-effect of fine fraction raw materials. *Mining Science*. 2020; 27: 7–18. Available from: doi: 10.37190/msc202701
13. Krivitskii B. A., Arsentieva K. S. On the method of determining the rheological properties of metals by torsion tests. *Izvestiya vuzov. Tsvetnaya metallurgiya = Izvestiya. Non-Ferrous Metallurgy*. 2014; 6: 34–37. (In Russ.)
14. Zhilin S. G., Komarov O. N., Potianikhin D. A., Sosnin A. A. Determination of logarithmic compaction equation parameters for the description of a process of uniaxial compaction of powder body made of polymeric material. *Vestnik Permskogo nacionalnogo issledovatel'skogo politekhnicheskogo universiteta. Mashinostroyeniye, materialovedeniye = Bulletin of the Perm National Research Polytechnic University. Mechanical engineering, materials science*. 2016; 18(4): 48–59. (In Russ.)
15. Noskov V. A., Baiul K. V. Investigations of the stress-strain state of fine-fraction mixtures during their briquetting. In: *Fundamental and applied problems of ferrous metallurgy: Collection of materials*. Dnepropetrovsk: Iron and Steel Institute NAS Ukraine Publishing; 2006; 13: 271–280. (In Russ.)

Received 12 May 2021

Information about authors:

Oleg A. Dorofeev – student, Department of Transport and Technological Systems in Construction and Mining, Pacific National University. E-mail: 2016105307@pnu.edu.ru; <https://orcid.org/0000-0002-7450-790X>

Evgenii A. Shishkin – PhD (Engineering), associate professor of the Department of Transport and Technological Systems in Construction and Mining, Pacific National University. E-mail: 004655@pnu.edu.ru; <https://orcid.org/0000-0003-4387-0228>

Anatolii A. Serebrennikov – DSc (Engineering), Professor, Chief researcher, Department of Transport and Technological Systems, Tyumen Industrial University. E-mail: serebrennikovaa@tyuiu.ru; <https://orcid.org/0000-0002-1649-5269>

Dmitrii E. Abramnikov – DSc (Engineering), Professor, professor of the Department of Construction Machines, Automation, and Electrical Engineering, Novosibirsk State University of Architecture and Civil Engineering. E-mail: abramnikov@sibstrin.ru; <https://orcid.org/0000-0002-7939-6014>

УДК 622.7

DOI: 10.21440/0536-1028-2021-5-87-98

Теоретическое обоснование силовых параметров валкового пресса

Дорофеев О. А.¹, Шишкин Е. А.¹, Серебренников А. А.², Абрамников Д. Э.³

¹ Тихоокеанский государственный университет, г. Хабаровск, Россия.

² Тюменский индустриальный университет, г. Тюмень, Россия.

³ Новосибирский государственный архитектурно-строительный университет, г. Новосибирск, Россия.

Реферат

Введение. Отходы углеобогащения являются привлекательным источником тепловой энергии. Ограниченное использование таких отходов связано с их низкой теплоотдачей. Для повышения теплоотдачи отходов их подвергают брикетированию с помощью прессового оборудования. Для брикетирования преимущественно используют валковый пресс, который характеризуется

высокой надежностью и сравнительно простой конструкцией. На качество получаемого брикета влияет усилие прессования рабочих элементов пресса.

Цель работы. Исследование направлено на установление связи между силовыми параметрами пресса и физико-механическими характеристиками прессуемого материала.

Методология. Исследование взаимодействия валков с прессуемым материалом производится в зоне прессования очага деформации. С учетом равномерности распределения давления материала вдоль образующих валков решается плоская задача. Для описания напряженно-деформированного состояния прессуемого материала использована упруго-вязко-пластическая реологическая модель как наиболее полно отражающая поведение реальной физической среды.

Результаты. Для принятой реологической модели получены аналитические зависимости давления на прессуемый материал от угла прессования для разных стадий деформирования материала. Установлена аналитическая связь усилия прессования и момента сопротивления вращению валка с конструктивными параметрами пресса, а также физико-механическими характеристиками прессуемого материала.

Выводы. Полученные зависимости позволяют более осознанно подходить к выбору силового оборудования пресса, обеспечивающего сжатие валков, а также к выбору привода необходимой мощности для получения качественных брикетов.

Ключевые слова: валковый пресс; конструктивные параметры; брикет; усилие прессования; момент сопротивления вращению; упруго-вязко-пластическая модель; угол прессования.

БИБЛИОГРАФИЧЕСКИЙ СПИСОК

1. Бажин В. Ю., Кусков В. Б., Кускова Я. В. Проблемы использования неостребованных угольных и других углеродсодержащих материалов в качестве энергетических брикетов // Уголь. 2019. № 4(1117). С. 50–54.
2. Кусков В. Б., Бажин В. Ю. Использование различных видов углеродсодержащего сырья для получения тепловой энергии // Записки Горного института. 2016. Т. 220. С. 582–586.
3. Xu R., Dai B., Wang W., Schenk J., Xue Z. Effect of iron ore type on the thermal behaviour and kinetics of coal-iron ore briquettes during coking // Fuel Processing Technology. 2018. Vol. 173. P. 11–20. DOI: 10.1016/j.fuproc.2018.01.006
4. Никишанин М. С., Загруднинов Р. Ш., Сеначин П. К. Брикетирование местных топлив и отходов для систем энергообеспечения в сельской местности // Ползуновский вестник. 2016. № 1. С. 88–95.
5. Manyuchi M., Mbohwa C., Muzenda E. Value addition of coal fines and sawdust to briquettes using molasses as a binder // South African Journal of Chemical Engineering. 2018. Vol. 26. P. 70–73. DOI: 10.1016/j.sajce.2018.09.004
6. Ефимов В. И., Никулин И. Б. Изготовление брикетов из угольных шламов обогатительных фабрик // ГИАБ. 2012. № 4-10. С. 26–32.
7. Fehse F., Rosin K., Hans-Werner S., Kim R., Spöttle M., Repke J.-U. Influence of briquetting and coking parameters on the lump coke production using non-caking coals // Fuel. 2017. Vol. 203. P. 915–923. DOI: 10.1016/j.fuel.2017.05.002
8. Большаков В. И., Маймур Б. Н., Баюл К. В. Научные основы технологии и оборудования для брикетирования техногенных отходов // Черная металлургия. 2009. № 8(1316). С. 54–59.
9. Wilczyński D., Berdychowski M., Talaśka K., Wojtkowiak D. Experimental and numerical analysis of the effect of compaction conditions on briquette properties // Fuel. 2021. Vol. 288. P. 119613. DOI: 10.1016/j.fuel.2020.119613
10. Носков В. А., Маймур М. Н., Петренко В. И. Разработка технологии производства коксовых брикетов на ОАО «Балгейкокс» // Металлургическая и горнорудная промышленность. 2005. № 3. С. 108–111.
11. Дьяконов О. М. Силовой расчет процесса брикетирования порошковых, стружковых и других сыпучих материалов // Литье и металлургия. 2019. № 3. С. 118–125.
12. Baiul K., Khudyakov A., Vashchenko S., Krot P., Solodka N. The experimental study of compaction parameters and elastic after-effect of fine fraction raw materials // Mining Science. 2020. Vol. 27. P. 7–18. DOI: 10.37190/msc202701
13. Кривицкий Б. А., Арсентьева К. С. К методике определения реологических свойств металлов испытаниями на кручение // Известия вузов. Цветная металлургия. 2014. № 6. С. 34–37.
14. Жилин С. Г., Комаров О. Н., Потянихин Д. А., Соснин А. А. Определение параметров логарифмического уравнения прессования для описания процесса одноосного уплотнения порошкового тела из полимерного материала // Вестник Пермского национального исследовательского политехнического университета. Машиностроение, материаловедение. 2016. Т. 18. № 4. С. 48–59.
15. Носков В. А., Баюл К. В. Исследования напряженно-деформированного состояния мелкофракционных шихт при их брикетировании // Фундаментальные и прикладные проблемы черной металлургии: сб. науч. тр. Днепродзержинск: ИЧМ НАН Украины, 2006. Вып. 13. С. 271–280.

Сведения об авторах:

Дорофеев Олег Алексеевич – студент кафедры транспортно-технологических систем в строительстве и горном деле Тихоокеанского государственного университета. E-mail: 2016105307@pnu.edu.ru; <https://orcid.org/0000-0002-7450-790X>

Шишкин Евгений Алексеевич – кандидат технических наук, доцент кафедры транспортно-технологических систем в строительстве и горном деле Тихоокеанского государственного университета. E-mail: 004655@pnu.edu.ru; <https://orcid.org/0000-0003-4387-0228>

Серебrenников Анатолий Александрович – доктор технических наук, профессор, главный научный сотрудник кафедры транспортных и технологических систем Тюменского индустриального университета. E-mail: serebrennikova@tyuiu.ru; <https://orcid.org/0000-0002-1649-5269>

Абраменков Дмитрий Эдуардович – доктор технических наук, профессор, профессор кафедры строительных машин, автоматики и электротехники Новосибирского государственного архитектурно-строительного университета. E-mail: abramenkov@sibstrin.ru; <https://orcid.org/0000-0002-7939-6014>

Для цитирования: Дорофеев О. А., Шишкин Е. А., Серебrenников А. А., Абраменков Д. Э. Теоретическое обоснование силовых параметров валкового пресса // Известия вузов. Горный журнал. 2021. № 5. С. 87–98 (In Eng.). DOI: 10.21440/0536-1028-2021-5-87-98

For citation: Dorofeev O. A., Shishkin E. A., Serebrennikov A. A., Abramnikov D. E. Theoretical justification of the roller press force parameters. *Izvestiya vysshikh uchebnykh zavedenii. Gornyi zhurnal = News of the Higher Institutions. Mining Journal*. 2021; 5: 87–98. DOI: 10.21440/0536-1028-2021-5-87-98